

## Environmental Chemical Contaminants

An Effective and Sensitive Environmental Pollutant  
Sensor for PymetrozineYudong Gao,<sup>1,\*</sup> Yapan Shi,<sup>1</sup> Huimin Li<sup>1</sup><sup>1</sup>Henan Bangtai Heli Management Consulting Co., Ltd, Environmental Monitoring Department, Zhengzhou 450000, China

\*Corresponding author's e-mail: gaoyudong0505@126.com

## Abstract

**Background:** Establishing an analytical method for detecting environmental pollutant pirimid using electrical analysis technology.**Objective:** Establishing a fast and effective environmental pollutant detection sensor.**Methods:** Prior to the modification, the bare GCE was pretreated with 0.1 μm alumina slurry and rinsed with water to provide a smooth and clean electrode surface. Afterwards, The fresh GCE surface was coated with 10 μL SWCNT suspension (0.5mg/mL) and dried under IR-lamp. Then the poly(L-arginine)/SWCNT modified GCE (poly(L-arginine)/SWCNT/GCE) was obtained by cyclic sweeping between –1500 mV and 2500 mV at the rate of 100 mV/s for 8 cycles in a PBS (pH 8.0) containing  $2.5 \times 10^{-3}$  mol/L L-arginine. This was the optimal depositional condition for fabricating the poly(L-arginine)/SWCNT/GCE from test. To evaluate the practical applicability of present method, farmland soil and river water were selected as sample.**Results:** In this study, we fabricated an electrochemical sensor to detect pymetrozine via combining SWCNT and electro-polymerizing poly(L-arginine) film modified GCE, as well as its electrochemical behavior. The as-prepared sensor features excellent electrocatalytic activities. It was also observed that the electrochemical property of the sensor was substantially improved because SWCNT afforded an enlarged active surface and accelerated electron transport. This sensor affords LSV in the linear range of 0.05~1.0 μM pymetrozine with a 17 nM low detection limit (S/N =3).**Conclusions:** A new and sensitive electrochemical sensor for pymetrozine determination was developed based on a single-walled carbon nanotubes (SWCNT) and poly(L-arginine) film. Results suggests that the poly(L-arginine)/SWCNT modified electrode exhibited a very low limit of detection.**Highlights:** The sensor enabled the measurement of pymetrozine in real samples obtained from farmland soil and river water. This work promoted the potential applications of amino acid materials and SWCNT in environmental pollution science.

The economic growth of a nation depends on its health and a disease-free environment. The chirality of agrochemicals and other industrial products is a big threat to human beings in terms of health problems and economic losses. It is well known that pesticides are a very important class of compounds used to kill pests (insects, rodents, and fungi) and unwanted plants (weeds; 1–5). They are also used to destroy vectors of many diseases such as mosquitoes, cockroaches, and termites. Different pesticides are frequently used in agriculture, horticulture, and municipal activities. Among the different pesticides, pymetrozine is used to manage different insects in farming, forestry, and horticulture (6–10).

The structure of pymetrozine, [4,5-dihydro-6-methyl-4-(3-pyridylmethyleneamino)-1,2,4-triazin-3(2H)-one], is shown in Figure 1(A)]. It is a new generation of second-generation nicotine-based high efficiency and low toxicity insecticides. It has gastric toxicity, contact toxicity, and systemic insecticide (11–14). So far, pymetrozine as a pesticide can be found widely in both soil and water. Its monitoring is very important due to its toxicity as an environmental pollutant (15–18). Hence, it is necessary to determine pymetrozine in the soil environment simply and quickly. Some analytical methods for pymetrozine have been proposed,

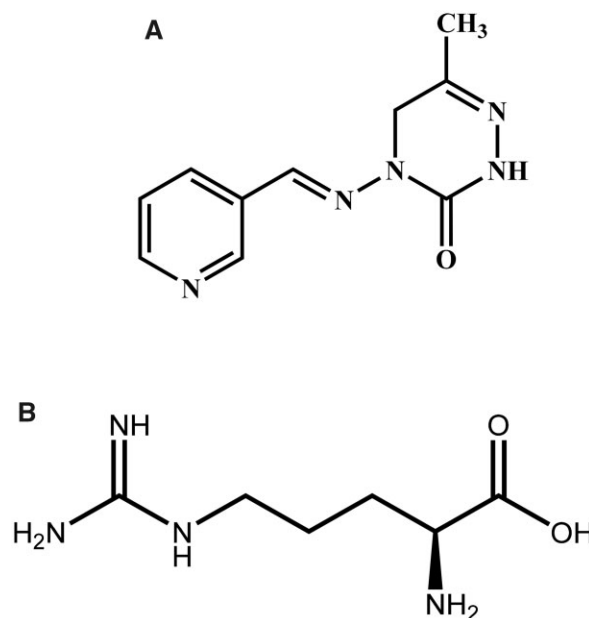


Figure 1. The chemical structure of pymetrozine (A) and L-arginine (B).

Received: 14 March 2020. Revised: 04 May 2020. Accepted: 12 May 2020

© The Author(s) 2020. Published by Oxford University Press on behalf of AOAC INTERNATIONAL. All rights reserved.

For permissions, please email: journals.permissions@oup.com

such as HPLC (19), GC (20), electronic spectroscopy (21), solid-phase extraction (SPE; 22), liquid-liquid extraction (23), and electroanalytical methods (12–15). Compared with other conventional methods, these electrochemical methods possess some unique and distinct advantages such as quicker responses, cost-effectiveness, cheap instrumentation, higher sensitivity, and easy preparation (24–40). A trend in analytical chemistry is developing the previously reported methods or introducing a new technique for improvement in the selectivity and sensitivity of chemical analysis methods. To the best of our knowledge, up to now there is no report on the application of poly(L-arginine)/single-walled carbon nanotubes (SWCNT)/GCE (glassy carbon electrode) to the detection of pymetrozine. The main aim of this study is electroanalytical detection of pymetrozine using a modified GCE. At the same time, it provides an idea for the sensitive detection of other environmental pollutants.

Amino acids are one of the numerous bioactive macromolecules used to construct biological organisms, and are the fundamental materials for building cells and repairing tissues. Due to its versatility and ease of preparation, L-arginine (structure shown in Figure 1(B)) is widely used to prepare voltammetric sensors (41, 42). L-arginine contains a carboxyl group and has electrostatic attraction for pymetrozine. In addition, carbon nanotubes (CNTs) possess good chemical stabilities, a high aspect ratio, large surface area, excellent electrical conductivity, and an ability to promote electron-transfer reactions. For these reasons, CNTs have been widely used in electrochemical sensors and environmental analytical chemistry (43–47). Nowadays, composite materials combining CNTs and poly amino acids have attracted increased attention due to the synergistic contribution of two or more functional components and many potential applications (48–58).

In this approach, a new voltammetric sensor made of composite materials, combining SWCNTs and an L-arginine modified glassy carbon electrode (poly(L-arginine)/SWCNT/GCE), was fabricated. In the present study, the fabrication, stability, and electrochemical properties of GCE modified SWCNT and poly(L-arginine) were investigated. To evaluate the utility of the modified electrode for analytical application, it was used for voltammetric detection of pymetrozine in real samples. This work promotes the potential applications of amino acid materials and SWCNTs in environmental pollution science.

## Experimental

### Apparatus and Reagents

An RST5000 electrochemical system (Zhengzhou Shiruisi Instrument Co. Ltd, Zhengzhou, China) was employed in experiments. A three-electrode system was used, consisting of a bare GCE (4 mm diameter) working electrode, a saturated calomel electrode (SCE), and a platinum (Pt) wire counter electrode. The pH Meter (Tianjin Sedleys Experimental Analytical Instrument Factory, Tianjin, China) was employed in experiments to adjust the pH value.

L-arginine and pymetrozine were obtained from Beijing Tanmo Quality Inspection Technology Co., Ltd (Beijing, China). A stock solution of pymetrozine ( $1 \times 10^{-2}$  mol/L) was prepared using high-purity water and stored at 4°C. SWCNTs were purchased from Nanjing Xianfeng Nanomaterials Technology Co., Ltd (Zhengzhou, China). Working solutions were prepared daily by diluting the stock solution with 0.1 mol/L H<sub>2</sub>SO<sub>4</sub>. All other reagents

were of analytical grade and were used without any further purification. High-purity water was used for all preparations.

### Fabrication of Poly(L-Arginine)/SWCNTs/GCE

Prior to modification, the bare GCE was pretreated with 0.3 μm alumina slurry and rinsed with water to provide a smooth and clean electrode surface. Afterwards, the electrode was sonicated in absolute ethanol for 5 s and allowed to dry naturally. The fresh GCE surface was coated with 10 μL SWCNT suspension (0.5 mg/mL) and dried under an IR lamp. Then the poly(L-arginine)/SWCNT modified GCE (poly(L-arginine)/SWCNT/GCE) was obtained by cyclic sweeping between –1500 and 2500 mV at the rate of 100 mV/s for eight cycles in a PBS (phosphate buffer solution) (pH 8.0) containing  $2.5 \times 10^{-3}$  mol/L L-arginine. This was the optimal depositional condition for fabricating the poly(L-arginine)/SWCNT/GCE from tests. For comparison, a poly(L-arginine)-modified GCE (denoted as poly(L-arginine)/GCE) was prepared using the same electro-polymerizing method and a SWCNT-modified GCE (called SWCNT/GCE) was established by depositing the above SWCNT suspension (10 μL) on the fresh GCE surface (42, 59, 60). Figure 2 shows the preparation of the modified electrode.

### Analytical Measurement Process

To obtain stable voltammograms, the prepared poly(L-arginine)/SWCNT/GCE was scanned between potentials of –500 and –1000 mV at a rate of 100 mV/s in H<sub>2</sub>SO<sub>4</sub> solution. When the cyclic voltammogram was steady, a certain volume of pymetrozine standard solution was added into the electrochemical cell. Then, the electrode was placed into the test solution and cyclic voltammetry (CV) or linear sweep voltammetry (LSV) was performed.

### Sample Solution Preparation

To evaluate the practical applicability of the method, farmland soil and river water were selected as samples. First, 0.5 g farmland soil was weighed and put into a 50 mL volumetric flask. Then, a certain amount of pymetrozine standard solution was added to the aforementioned volumetric flask and fix the volume with water. Last, the sample was pretreated by ultrasonication for 30 min. After 10 min centrifugation at 10 000 revolutions per minute (rpm), the clear liquid phase was collected for further analysis.

## Results and Discussion

### Electrochemical Sensor Response of Pymetrozine

To characterize the modified electrode, electrochemical impedance spectroscopy (EIS) was carried out in an electrolyte containing  $5 \times 10^{-3}$  mol/L [Fe(CN)<sub>6</sub>]<sup>3-/4-</sup> and 0.1 mol/L KCl. The Nyquist plot of EIS has two parts, the linear segment at lower frequency and the semicircle part at higher frequency, which mark the diffusion-controlled process and the electron-transfer-limited process, respectively. The charge transfer resistance (R<sub>ct</sub>) can be obtained from the semicircle diameter. Figure 3 is the enlargement of the Nyquist plots (Z' versus -Z'') at bare GCE and the modified electrodes in the high-frequency region. The R<sub>ct</sub>s of the four electrodes were 55.32 Ω at the bare GCE (a), 27.45 Ω at the SWCNT/GCE (b), 25.1 Ω at the poly(L-arginine)/GCE (c), and 18.11 Ω at the poly(L-arginine)/SWCNTs/GCE (d). These data demonstrated that impedance decreased when SWCNTs were added on the GCE or L-arginine polymerized on the GCE. This was the

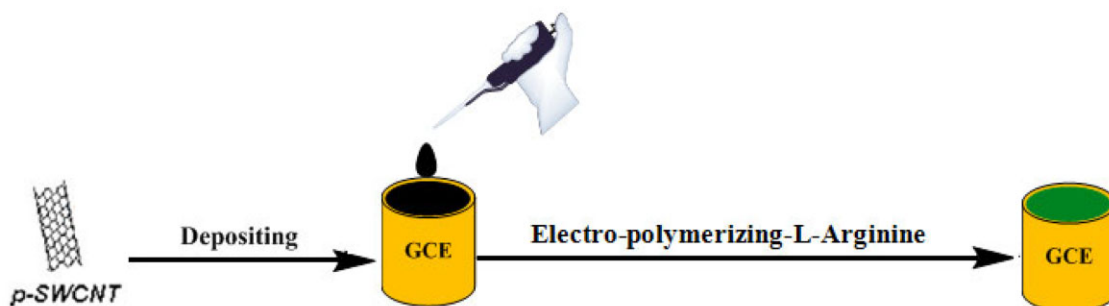


**Figure 2.** Schematic illustration for the stepwise preparation of poly(L-arginine)/SWCNT/GCE.

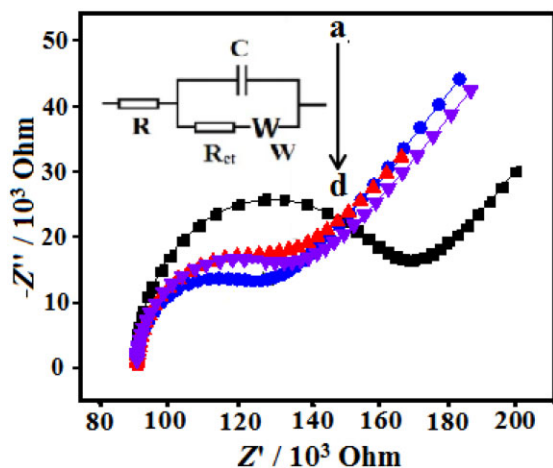


**Figure 3.** The Nyquist plots of EIS in the high-frequency region at: (a) GCE, (b) SWCNT/GCE, (c) poly(L-arginine)/GCE, (d) poly(L-arginine)/SWCNT/GCE. Supporting electrolyte:  $5 \times 10^{-3}$  mol/L  $K_3[Fe(CN)_6]/K_4[Fe(CN)_6]$  (1:1) with 0.1 mol/L KCl solution; Working potential: 0.285 V; Frequency: 1 M Hz to 0.01 Hz.

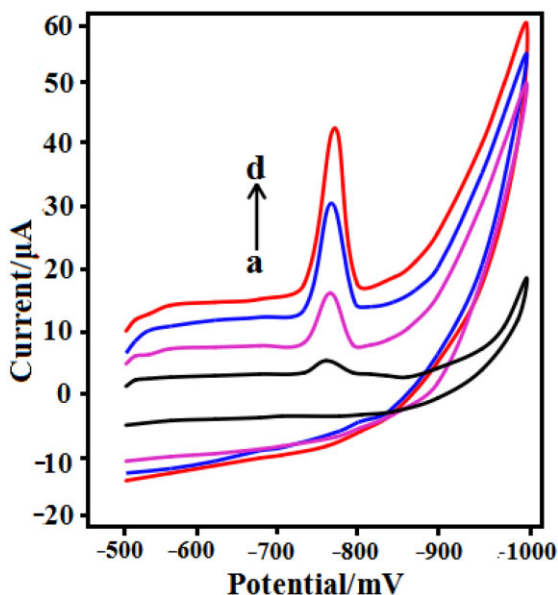


**Figure 4.** Cyclic voltammograms of pymetrozine ( $5.0 \times 10^{-5}$  mol/L) at the bare GCE (curve a), SWCNT/GCE (curve b), poly(L-arginine)/GCE (curve c), and poly(L-arginine)/SWCNT/GCE (curve d). Supporting electrolyte: 0.1 mol/L  $H_2SO_4$  (pH 1.0); scan rate: 0.1 V/s.

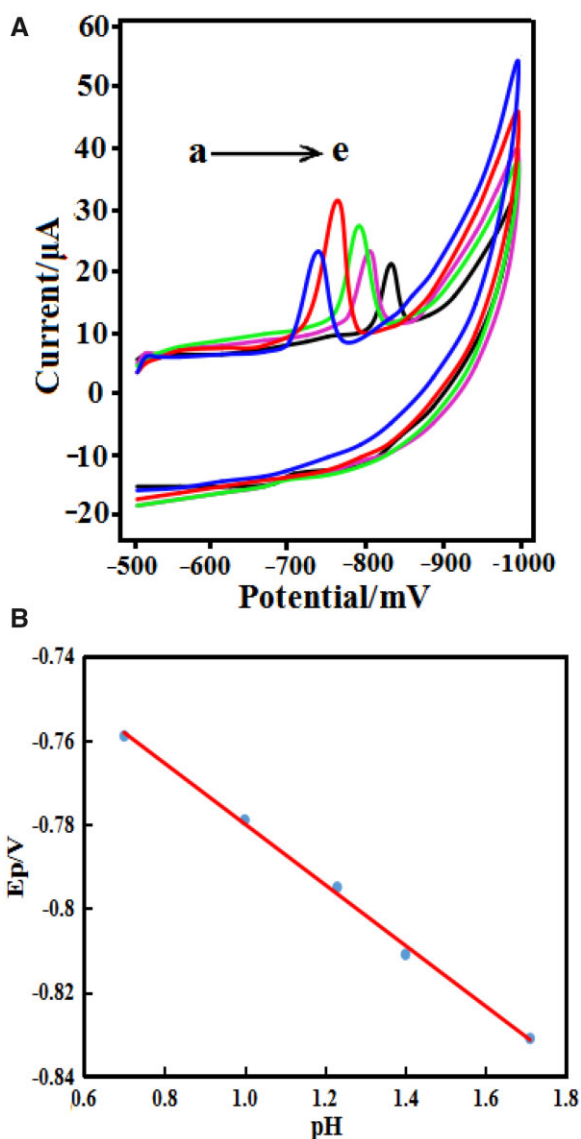
result of the conductivity of SWCNTs and the high electrochemical activity of L-arginine. At the poly(L-arginine)/SWCNT/GCE, the resistance was reduced sharply compared to the bare GCE, an attribute of SWCNT and poly(L-arginine) functioning together.

Figure 4 shows the cyclic voltammograms in the presence of 50.0  $\mu$ M pymetrozine with the bare GCE (curve a), SWCNT/GCE (curve b), poly(L-arginine)/GCE (curve c), and poly(L-arginine)/SWCNT/GCE (curve d). There is a flat peak pattern on the curves, illustrating that a mild redox reaction even occurred at the bare GCE. When the poly(L-arginine)/GCE and the SWCNT/GCE served as working electrodes, the peak value increased slightly. The most sensitive voltammetric response of pymetrozine at the poly(L-arginine)/SWCNT/GCE may be from a synergistic effect of the larger specific surface area and better accumulation capability of poly(L-arginine)/SWCNT. Then, a sensitive electroanalytical method was proposed based on the poly(L-arginine)/SWCNT/GCE as the voltammetric sensor for pymetrozine.

### Effect of Solution pH

To get the best response of pymetrozine ( $1.0 \times 10^{-6}$  mol/L) at the poly(L-arginine)/SWCNT/GCE, the influence of different supporting electrolytes were investigated by CV, including 0.1 mol/L phosphate buffer solution, acetate buffer solution, Britton–Robinson, and  $H_2SO_4$  solution. After consideration of the peak shape and sensitivity, 0.1 mol/L  $H_2SO_4$  was chosen as supporting electrolyte in the following experiments.

To optimize the determination conditions and study the reaction characteristics of pymetrozine at the poly(L-arginine)/SWCNT/GCE, the influence of the solution pH on the reduction reaction of poly(L-arginine)/SWCNT was studied in the pH range 0.7–1.71. As shown in Figure 5A, the cathodic peak current changed gradually and the potential was negatively shifted by increasing the solution pH value. This indicated that there were protons taking part in the electrode reaction of pymetrozine. The peak potential ( $E_p$ ) and pH value had a good linear relationship with a correlation equation of:  $E_p$  (V) =  $-0.068\text{pH} - 0.7922$ ,  $R = 0.998$  (Figure 5B). According to the Nernst equation, this slope of 0.068 V/pH was almost same as the theoretical value (0.059 V/pH), which suggests that an equal number of electrons and protons take part in the pymetrozine reduction process at the electrode surface. According to the above results and previous reports (12–15), it appears that two electrons and two protons are involved in the reduction reaction of pymetrozine. Therefore, the feasible mechanism for the electrochemical behavior of pymetrozine at the poly(L-arginine)/SWCNT/GCE may be described as shown in Figure 6. Moreover, the cathodic peak currents of pymetrozine also changed within the investigated pH range. The



**Figure 5.** (A) Cyclic voltammograms of pymetrozine ( $5.0 \times 10^{-5}$  mol/L) at the sensor in  $\text{H}_2\text{SO}_4$  with different pH (a to e: 0.7, 1.0, 1.23, 1.4, 1.71). Scan rate: 0.1 V/s. (B)  $E_p$ -pH relationship.

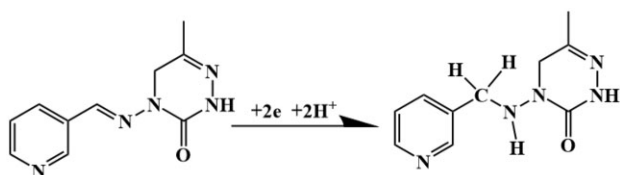


**Figure 6.** Possible reduction reaction mechanism of pymetrozine.

maximum peak current appeared at pH 1.0 from the  $\text{H}_2\text{SO}_4$  solution, which was selected as the optimal pH to detect pymetrozine with the highest sensitivity.

## Analytical Applications and Method Validation

(a) *Influence of accumulation time.*—In consideration of the detection sensitivity of pymetrozine on the sensor surface, a

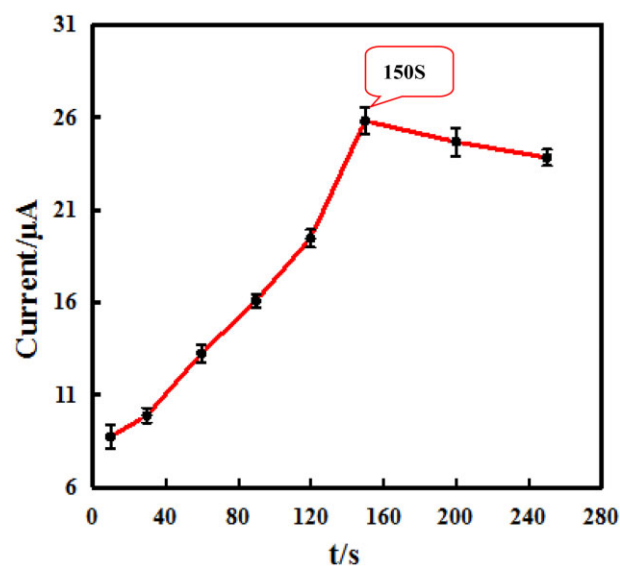


**Figure 7.** The relation between the peak currents of pymetrozine ( $1.0 \times 10^{-6}$  mol/L) and the accumulation time (10, 30, 60, 90, 120, 150, 200, and 250 s). Supporting electrolyte: 0.1 mol/L  $\text{H}_2\text{SO}_4$ , pH = 1.0, scan rate: 0.1 V/s.

step of accumulation has a significant effect on the detection sensitivity. The relationship was recorded between accumulation time and peak currents in a pymetrozine solution ( $1.0 \times 10^{-6}$  mol/L) via LSV. Figure 7 shows that with the increase in accumulation time (10~250 s), the responding peak currents gradually up to 150 s and subsequently slowly increased. Considering the detection sensitivity and linear range, an accumulation time of 150 s was chosen to set up the calibration curve in subsequent experiments.

(b) *Calibration curve, LOD, reproducibility, and stability.*—With regard to the pymetrozine resultant peak currents at the poly(L-arginine)/SWCNT/GCE, pymetrozine was quantitatively analysed in electrolyte. We also utilized the modified electrode as the working electrode within a range of pymetrozine concentration. Figure 8A shows the superimposed voltammograms of different pymetrozine concentrations using LSV. For the experimental results, peak current was recorded and used as the detected signal. A good linear relationship was obtained between the peak current ( $i_p$ ) and pymetrozine concentrations (as shown in Figure 8B). The linear regression equation was  $i_p$  ( $\mu\text{A}$ ) = 19.36 C ( $\mu\text{M}$ ) + 0.4361 ( $R^2 = 0.9983$ ). From the slope of 19.36  $\mu\text{A}/\mu\text{M}$ , the LOD was estimated to be 17 nM ( $S/N=3$ ) using the following method (61, 62):  $\text{LOD} = \text{SD}_{\text{background}}/S$ , where S = slope or sensitivity and SD = standard deviation. A comparison of the poly(L-arginine)/SWCNT/GCE with other sensors for pymetrozine determination is given in Table 1.

The repeatability and stability of the sensor were evaluated by LSV in pymetrozine solution ( $1.0 \times 10^{-6}$  mol/L). For one electrode, five parallel measurements were carried out under identical conditions, and an RSD of 1.9% was estimated. Meanwhile, the obtained RSD was 2.8% from five parallel fabricated poly(L-arginine)/SWCNT/GCEs, revealing a good reproducibility. In order to test the poly(L-arginine)/SWCNT/GCE stability, we maintained our sensor at 4°C for

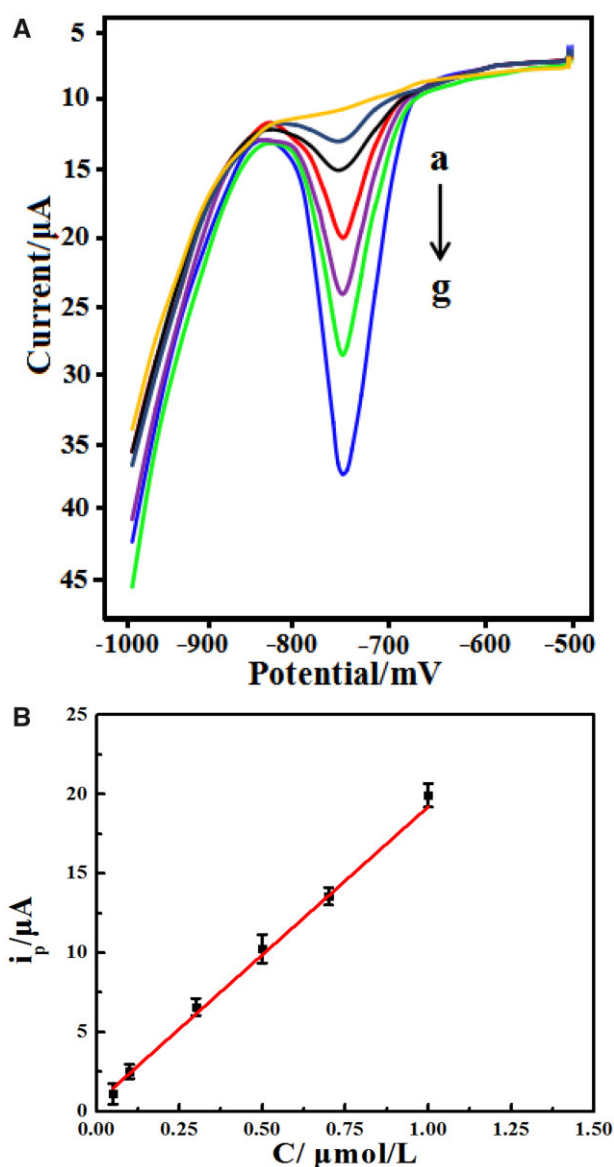


**Figure 8.** (A) Superimposed LSV curves of different pymetrozine concentrations obtained in 0.1 mol/L H<sub>2</sub>SO<sub>4</sub> (pH 1.0). Pymetrozine concentration (a to g): 0, 5.0 × 10<sup>-8</sup>, 1.0 × 10<sup>-7</sup>, 3.0 × 10<sup>-7</sup>, 5.0 × 10<sup>-7</sup>, 7.0 × 10<sup>-7</sup>, and 1.0 × 10<sup>-6</sup> mol/L. (B) Calibration plot of peak current versus pymetrozine concentrations.

14 days and recorded the LSV of a solution consisting of 1.0 μM of pymetrozine in order to compare to the LSV achieved prior to the immersion. Results showed no change in the pymetrozine peak. Moreover, the current declined by approximately 96.7% in the signal compared with the initial responses, implying a reasonable stability for the poly(L-arginine)/SWCNT/GCE. The renewal of the poly(L-arginine)/SWCNT/GCE was easily achieved in H<sub>2</sub>SO<sub>4</sub> solution by successive sweeping of two cycles between -500 mV and -1000 mV to give a regenerated electrode surface. This step was repeated several times and the result of eight measurements is shown in Table 2 with an RSD of current response was 2.6%.

- (c) **Selectivity studies.**—The influence of various potentially interfering substances for determination of 1.0 × 10<sup>-6</sup> mol/L pymetrozine was studied by LSV. The tolerance limit for foreign species was taken as the largest amount yielding a relative error ≤5% for the determination of pymetrozine. As shown in Figure 9, the results indicated that 100-fold of Al<sup>3+</sup>, SO<sub>4</sub><sup>2-</sup>, Zn<sup>2+</sup>, NO<sub>3</sub><sup>-</sup>, Cr<sup>6+</sup>, Cr<sup>3+</sup>, and Cd<sup>2+</sup>, 20-fold of citric acid, ascorbic acid, quinclorac, thiamethoxam, and imidacloprid, and 10-fold uric acid had almost no influence on the determination. This proves clearly the reasonable selectivity of the proposed method.
- (d) **Determination of pymetrozine in real samples and recovery.**—In order to prove the feasibility of the analysis method, farmland soil and river water were chosen as real samples. The treatment processes for the real samples is described in Experimental and the detection results are listed in Table 3. The content of pymetrozine in farmland soil was 0.0026 mg/g and its RSD was 1.4% for three repeated measurements. Additionally, the recoveries for pymetrozine in farmland soil sample were calculated to be in the range of 96–103%. No pymetrozine was detected in river water samples, so some standard pymetrozine was added to test recovery. These data demonstrated that the proposed method has good accuracy for the determination of pymetrozine.

## Conclusions

Pymetrozine plays an important role in agriculture safety supervision. Accurate and rapid detection of pymetrozine in real samples counts for much as this is the significant prerequisite for its

**Table 1.** Comparison of different voltammetric sensors for the determination of pymetrozine

Modified electrode	Linear range, mol/L	LOD, mol/L	Voltammetric technique	Ref.
Dropping mercury electrode	4.97 × 10 <sup>-7</sup> ~ 7.35 × 10 <sup>-6</sup>	1.48 × 10 <sup>-7</sup>	DPV <sup>a</sup>	(12)
EPGCE <sup>b</sup>	1.0 × 10 <sup>-7</sup> ~ 5.0 × 10 <sup>-6</sup>	8.0 × 10 <sup>-8</sup>	LSV <sup>c</sup>	(13)
Mercury meniscus modified silver solid amalgam electrode	2.0 × 10 <sup>-7</sup> ~ 1.0 × 10 <sup>-4</sup>	5.4 × 10 <sup>-8</sup>	DPV	(14)
PABA-ZnNP-fMWCNT-IL-CPE <sup>d</sup>	1.0 × 10 <sup>-8</sup> ~ 5.0 × 10 <sup>-6</sup>	8.3 × 10 <sup>-10</sup>	AdSWV <sup>e</sup>	(15)
Poly(L-arginine)/SWCNT/GCE	5.0 × 10 <sup>-8</sup> ~ 1.0 × 10 <sup>-6</sup>	1.7 × 10 <sup>-8</sup>	LSV	This work

<sup>a</sup> DPV = Differential pulse voltammetry.

<sup>b</sup> EPGCE = Electrochemically pretreated glassy carbon electrode.

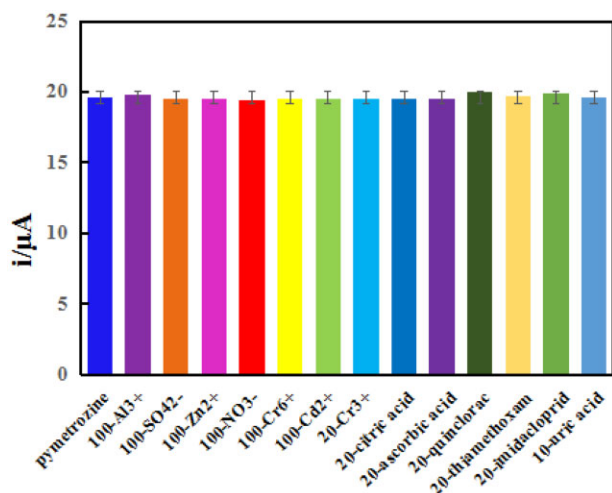
<sup>c</sup> LSV = Linear sweep voltammetry.

<sup>d</sup> PABA-ZnNP-fMWCNT-IL = Polyaminobenzoic acid functionalized zinc nanoparticles supported on composite of functionalized multiwalled carbon nanotubes and ionic liquid.

<sup>e</sup> AdSWV = Adsorptive square wave voltammograms.

**Table 2.** Repeatability experiment of modified electrode.

Number	Peak current, $\mu\text{A}$	RSD, %
1	16.2	2.6
2	16.2	
3	15.7	
4	15.2	
5	15.5	
6	15.4	
7	15.1	
8	15.6	

**Figure 9.** Column chart of the peak current of  $1 \times 10^{-6}$  mol/L pymetrozine and co-exist with other metal ions or organic compounds.**Table 3.** Analysis results and recovery of real samples

Sample	Results in detection solution, $\mu\text{M}$	Added, $\mu\text{M}$	Found, $\mu\text{M}$	RSD, % <sup>a</sup>	Recovery, %	Sample content, mg/g
Farmland soil	0.6	0.2	0.81	2.1	103	0.0026
		0.4	1.0	1.5	96	
		0.6	1.2	2.2	101	
River water	ND <sup>b</sup>	0.1	0.11	1.6	110	ND
		0.3	0.29	2.3	97	
		0.5	0.52	1.4	104	

<sup>a</sup> Average value of three replicate measurements.<sup>b</sup> ND = Not detected.

effective monitoring. In this study, we fabricated an electrochemical sensor to detect pymetrozine via combining SWCNTs and an electro-polymerizing poly(L-arginine) film-modified GCE, as well as its electrochemical behavior. The as-prepared sensor has excellent electrocatalytic activities. It was also observed that the electrochemical property of the sensor was substantially improved because SWCNTs afforded an enlarged active surface and accelerated electron transport. This sensor affords LSV in the linear range of 0.05~1.0  $\mu\text{M}$  pymetrozine with a 17 nM low LOD ( $S/N=3$ ). Many important features, including decent anti-interference, reproducibility, stability, and reliability, were also observed. Importantly, the sensor enabled the measurement of pymetrozine in real samples obtained from farmland soil and river water, thus demonstrating its practical potential as a pymetrozine analytical detector.

## Conflicts of Interest

No potential conflict of interest was reported by the authors.

## References

- Ali, I., Gupta, V.K., & Aboul-Enein, H.Y. (2003) *Curr. Sci.* **84**, 152–156
- Bhanti, M., & Taneja, A. (2007) *Chemosphere* **69**, 63–68.
- Nile, A.S., Kwon, Y.D., & Nile, S.H. (2019) *Environ. Sci. Pollut. Res. Int.* **26**, 1–5
- Basheer, A.A. (2017) *Chirality* **85**, 1–3
- Ali, I. (2012) *Chem. Rev.* **10**, 5073–5091.
- Ali, I., Asim, M., & Khan, T.A. (2013) *Int. J. Environ. Sci. Technol.* **10**, 377–384
- Ali, I., & Aboul-Enein, H.Y. (2002) *Environ. Toxicol.* **17**, 329–333
- Basheer, A.A., & Ali, I. (2018) *Chirality* **30**, 1088–1095
- Ali, I., Singh, P., Rawat, M.S.M., & Badoni, A. (2008) *India J. Environ. Protect. Sci.* **2**, 47–51
- Lupi, L., Bedmar, F., Wunderlin, D.A., & Miglioranza, K.S.B. (2019) *Environ. Earth Sci.* **78**, 569–572
- Sechser, B., Reber, B., & Bourgeois, F. (2002) *J. Pest Sci.* **75**, 72–77
- Mercan, H., Yilmaz, E., & Inam, R. (2007) *J. Hazard. Mater.* **141**, 700–706
- Jia, D.L., Gao, J., Wang, L., Gao, Y.D., & Ye, B.X. (2015) *Anal. Methods* **7**, 9100–9107
- Renáta, Š., Lenka, J.B., Michaela, K., & Michaela, Š. (2016) *Anal. Lett.* **49**, 4–18.
- Khan, I., Bano, M., Khan, G.A., & Khan, F. (2018) *Mater. Sci. Eng.* **238-239**, 83–92
- Shen, G.Q., Hu, X., & Hu, Y.A. (2009) *J. Hazard. Mater.* **164**, 497–501
- Zhang, Y.F., Zhang, L., Xu, P., Li, J.Z., Wang, H.L., & Environ, M. (2015) *Assess* **187**, 78–85
- Sabine-Karen, L., Julien, M., & Enrique, B. (2016) *Environ. Sci. Pollut. Res. Int.* **24**, 1–7
- Zhang, X., Cheng, X.S., & Wang, C.Q. (2007) *Ann. Chim. (Rome)* **97**, 295–301
- Jang, J., Rahman, M.M., & KoA, A.Y. (2014) *Food Chem.* **146**, 448–454
- Zhang, Y., Zhou, H., & Jiang, Z.J. (2011) *Spectrochim. Acta, Part A* **83**, 112–119
- Shan, J., Wang, Q., Zhang, Z., & Han, J. (2015) *Asian J. Chem.* **27**, 1537–1539
- Hong, J.H., Lee, C.R., Lim, J.S., Lee, K.S., & Bull, E. (2011) *Contam. Toxicol.* **87**, 649–652
- Shamsipur, M., Roushani, M., & Pourmortazavi, S.M. (2014) *Cent. Eur. J. Chem.* **12**, 1091–1099
- Shamsipur, M., Roushani, M., Mansouri, G., & Chin, J. (2013) *Chem. Soc. 60*, **171-178**
- Roushani, M., Shamsipur, M., & Pourmortazavi, S.M. (2012) *J. Appl. Electrochem.* **42**, **1005-1011**
- Roushani, M., Nezhadali, A., & Jalilian, Z. (2018) *Microchim. Acta* **185**, 558–565
- Roushani, M., Nezhadali, A., & Jalilian, Z. (2018) *Mikrochim. Acta* **185**, 551–557
- Shahdost-fard, F., Roushani, M., & Azadbakht, A. (2017) *Anal. Biochem.* **534**, 78–85
- Valipour, A., & Roushani, M. (2017) *Microchim. Acta* **184**, 2015–2022
- Roushani, M., & Ghanbari, K. (2018) *Anal. Methods* **10**, 5197–5204
- Taherkhani, A., Jamali, T., Hadadzadeh, H., Karimi-Maleh, H., Beitollahi, H., Taghavi, M., & Karimi, F. (2014) *Ionic* **20**, 421–429

33. Kazemipour, M., Ansari, M., Mohammadi, A., Beitollahi, H., & Ahmadi, R. (2009) *J. Anal. Chem.* **64**, 65–70
34. Moghaddam, H.M., Beitollahi, H., Tajik, S., Malakootian, M., & Maleh, H.K. (2014) *Environ. Monit. Assess.* **186**, 7431–7441
35. Moghaddam, H.M., Tajik, S., & Beitollahi, H. (2019) *Food Chem.* **286**, 191–196
36. Beitollahi, H., Movahedifar, F., Tajik, S., & Jahani, S. (2019) *Electroanalysis* **31**, 1195–1203
37. Ganjali, M.R., Salimi, H., Tajik, S., Beitollahi, H., Rezapour, M., & Larijani, B. (2017) *Int. J. Electrochem. Sci.* **12**, 5243–5249
38. Tajik, S., & Beitollahi, H. (2019) *Anal. Bioanal. Chem. Res.* **6**, 171–181
39. Khalilzadeh, M.A., Tajik, S., Beitollahi, H., & Venditti, R.A. (2020) *Ind. Eng. Chem. Res.* **59**, 4219–4223
40. Beitollahi, H., Tajik, S., Asadi, M.H., & Biparva, P. (2014) *J. Anal. Sci. Technol.* **5**, 1–9
41. Ghasem, K.N., Zeynab, K., & Dorraji, P.S. (2017) *Sens. Lett.* **15**, 282–288
42. Qiao, W.H., Wang, L., Li, H.H., Li, G.P., Li, J.J., & Ye, B.X. (2015) *Talanta* **144**, 726–733
43. Matlou, G.G., Nkosi, D., Pillay, K., & Arotiba, O. (2016) *Sens. Bio-Sens. Res.* **10**, 27–33
44. Brahman, P.K., Suresh, L., Reddy, K.R., & Bondili, J.S. (2017) *RSC Adv.* **7**, 37898–37907
45. Khan, I., Pandit, U.J., Wankar, S., Das, R., & Limaye, S.N. (2017) *Ionics* **23**, 1293–1308
46. Khan, I., Pandit, U.J., & Limaye, S.N. (2017) *Electroanalysis* **29**, 2423–2436
47. Pandiyaraj, K., & Shanmugam, S.K. (2018) *Electroanalysis* **30**, 445–452
48. Dali, M., Zinoubi, K., & Chrouda, A. (2018) *J. Electroanal. Chem.* **813**, 9–19
49. Ye, Z., Yang, L.X., Wen, J.G., & Ye, B.X. (2015) *Anal. Methods* **7**, 2855–2861
50. Wang, W.J., Wang, L., Zou, L.N., Li, G.P., & Ye, B.X. (2016) *Talanta* **150**, 346–354
51. Liu, J., Li, Y.F., Song, G., Zhang, K., & Ye, B.X. (2014) *Intern. J. Environ. Anal. Chem.* **97**, 884–900
52. Lisebo, P., Carla, G.C., & Madalina, M.B. (2019) *Anal. Lett.* **5**, 1–6
53. Alejandro, G., Fabiana, G., Marcos, E., & Gustavo, A.R. (2016) *RSC Adv.* **6**, 13469–13477
54. Wang, Y., Ding, Y., Li, L., & Hu, P. (2018) *Talanta* **178**, 449–457
55. Alizadeh, T., Mirzaee, S., & Rafiei, F. (2017) *Int. J. Environ. Anal. Chem.* **97**, 1283–1297
56. Hadi, M., Bayat, M., Mostanzadeh, H., Ehsani, A., & Yeganeh-Faal, A. (2018) *Int. J. Environ. Anal. Chem.* **98**, 197–214
57. Vinay, M.M., Arthoba Nayaka, Y., Purushothama, H.T., Yathisha, R.O., Basavarajappa, K.V., & Manjunatha, P. (2019) *Int. J. Environ. Anal. Chem.* **99**, 1553–1564
58. Damiri, S., Pouretdal, H.R., & Heidari, A. (2016) *Int. J. Environ. Anal. Chem.* **96**, 11–15
59. Hua, A.Y., & Huang, J.Z. Song, Z.R. & Song, L. (2014) *Sens. Transducers* **175**, 1–8
60. Wu, J.J., Wang, L., Wang, Q.Q., Zou, L.N., & Ye, B.X. (2016) *Talanta* **150**, 61–70
61. Khan, I., Pandit, U.J., Wankar, S., & Limaye, S.N. (2017) *Environ. Nanotechnol. Monitor. Manage.* **7**, 64–72
62. Khana, I., Banoa, M., Khanb, G.A., & Khan, F. (2018) *Mater. Sci. Eng. B* **238**, 83–90